Cell, Vol. 121, 823–835, June 17, 2005, Copyright ©2005 by Elsevier Inc. DOI 10.1016/j.cell.2005.03.032

Identification of Bronchioalveolar Stem Cells in Normal Lung and Lung Cancer

Carla F. Bender Kim,[1] Erica L. Jackson,[1,3] Amber E. Woolfenden,[1,2] Sharon Lawrence,[1] Imran Babar,[2] Sinae Vogel,[1] Denise Crowley,[1] Roderick T. Bronson,[4] and Tyler Jacks[1,2,*]

[1]Center for Cancer Research and Department of Biology

[2]Howard Hughes Medical Institute

Massachusetts Institute of Technology

Cambridge, Massachusetts 02139

Summary

Injury models have suggested that the lung contains anatomically and functionally distinct epithelial stem cell populations. We have isolated such a regional pulmonary stem cell population, termed *b*ronchio*a*lveolar *s*tem *c*ells (BASCs). Identified at the bronchioalveolar duct junction, BASCs were resistant to bronchiolar and alveolar damage and proliferated during epithelial cell renewal in vivo. BASCs exhibited self-renewal and were multipotent in clonal assays, highlighting their stem cell properties. Furthermore, BASCs expanded in response to oncogenic K-ras in culture and in precursors of lung tumors in vivo. These data support the hypothesis that BASCs are a stem cell population that maintains the bronchiolar Clara cells and alveolar cells of the distal lung and that their transformed counterparts give rise to adenocarcinoma. Although bronchiolar cells and alveolar cells are proposed to be the precursor cells of adenocarcinoma, this work points to BASCs as the putative cells of origin for this subtype of lung cancer.

Introduction

The pulmonary system contains a variety of epithelial cell populations that each reside in distinct anatomical locations. Basal, secretory, and ciliated cells line the trachea and the proximal conducting airways; neuroendocrine cells are present in small numbers. The nonciliated, columnar Clara cells comprise the majority of the bronchiolar and terminal bronchiolar epithelium in mice, and alveolar type I (AT1) and type II (AT2) cells constitute the alveolar epithelium (Bannister, 1999).

Injury models have suggested that functionally distinct epithelial stem cell populations exist in precise anatomical locations in the lung (Otto, 2002). A putative tracheal and proximal conducting airway stem cell niche has been identified by resistance to the detergent polidocanol and sulfur dioxide (Borthwick et al., 2001). Bleomycin administration results in AT1 cell injury, and it has been proposed that AT2 cells repair the damaged alveolar epithelium (Aso et al., 1976). Naphthalene, a pollutant that specifically ablates Clara cells, has been used to identify two distinct stem cell niches. In proximal airways, naphthalene-resistant Clara cells are closely associated with neuroendocrine bodies, whereas resistant cells are found at the junction between the conducting and respiratory epithelium (the bronchioalveolar duct junction, or BADJ) in terminal bronchioles (TBs) (Giangreco et al., 2002; Hong et al., 2001; Reynolds et al., 2000a; Reynolds et al., 2000b). "Side population" cells exhibiting Hoechst dye efflux properties similar to those of hematopoietic stem cells have been isolated from lung (Giangreco et al., 2003; Goodell et al., 1996; Summer et al., 2003). Despite these advances, methods to isolate cells from putative stem cell niches in the lung and functional tests for such populations have not been reported.

Just as our understanding of lung stem cell biology is limited, the identity of the cell of origin in lung tumorigenesis is also largely unknown. This is due in part to the predominantly advanced stage of disease in most patients at the time of diagnosis (Minna et al., 2002). Interestingly, many of the subtypes of non-small cell lung carcinoma share characteristics with differentiated cells found in the distinct locations in which the tumors arise. For example, squamous cell carcinomas exhibit keratinization like mature epithelial cells in the trachea and proximal airways and generally arise in bronchi, whereas most adenocarcinomas display Clara or AT2 cell markers and are generally peripheral or endobronchial (Rosai and Sobin, 1995). However, whether the cancers arise from these differentiated cell compartments or from stem or progenitor cells has not been established.

We previously developed a "Lox-Stop-Lox" *K-ras* conditional mouse strain (referred to as *LSL-K-ras G12D*), in which expression of oncogenic *K-ras* is spatially and temporally controlled by a removable transcriptional termination ("stop") element (Jackson et al., 2001). Intranasal infection with recombinant adenoviral Cre (AdCre) results in deletion of the stop element, producing the *Lox-K-ras* allele that expresses *K-ras G12D*. *Lox-K-ras* mice develop atypical adenomatous hyperplasias (AAH; hyperproliferations of AT2 cells) that appear to progress to adenomas and then overt adenocarcinomas (Jackson et al., 2001). This progression, together with the observation that *Lox-K-ras* adenocarcinomas were positive for the AT2 cell-specific marker prosurfactant apoprotein-C (SP-C), was consistent with previous studies that implicated AT2 cells as the target cells in rodent and human lung adenocarcinomas. However, evidence in other murine models and human specimens points to Clara cells as the cell of origin of adenocarcinoma (Dermer, 1982; Gunning et al., 1991; Mason et al., 2000; Mori et al., 1993; Mori et al., 2001; Thaete and Malkinson, 1991; Wikenheiser et al., 1992).

During analysis of *Lox-K-ras* tumors, we identified a novel cell type, termed double-positive cells (DPCs). DPCs expressing both SP-C and the Clara cell-specific marker CCA (also known as CC10 or CCSP) were found

*Correspondence: tjacks@mit.edu

[3]Present address: Department of Neurological Surgery, University of California, San Francisco, San Francisco, California 94143.

[4]Present address: Department of Biomedical Sciences, Tufts University Veterinary School, North Grafton, Massachusetts 05136.

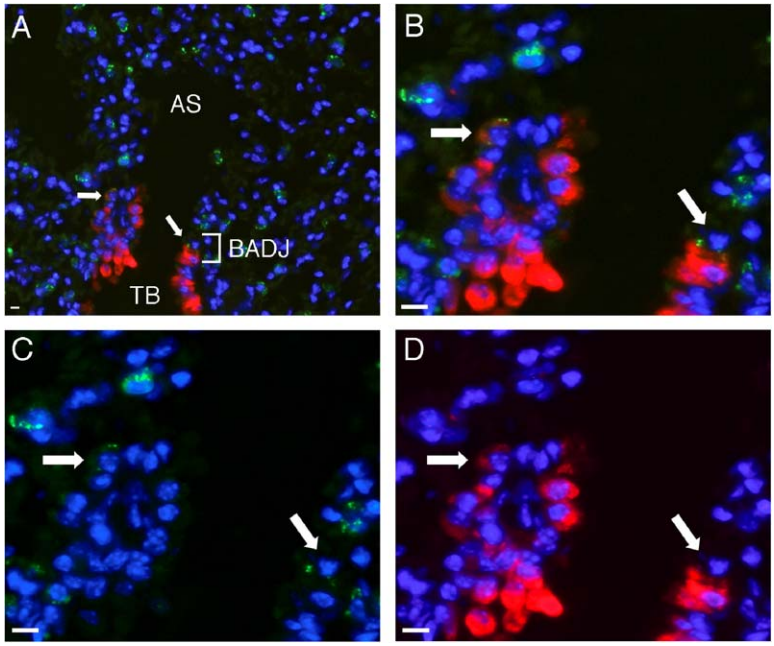

Figure 1. Identification of BASCs in Normal Lung

BASCs (arrows) are located at the bronchioalveolar duct junction (BADJ, brackets), the branch point between a terminal bronchiole (TB) lined with Clara cells positive for CCA and the alveolar space (AS) lined with alveolar epithelium including AT2 cells positive for SP-C. IF for DAPI (blue), CCA (red), and SP-C (green) is shown.

(A) 400× image, merge.

(B–D) Zoom of 400× image to highlight the BADJ region. Merge (B), green channel only (C), and red channel only (D). Scale bars, 10 μm.

in adenomas, particularly in lesions continuous with bronchiolar hyperplasia (Jackson et al., 2001). We now show that counterparts of the SP-C^{pos} CCA^{pos} *Lox-K-ras* DPCs, renamed BASCs, exist in normal lung, function in lung homeostasis, and possess characteristics of regional stem cells. Furthermore, we provide evidence that BASCs are the cells of origin of adenocarcinoma.

Results

CCA-Positive, SP-C-Positive Cells in Normal Adult Lung

DPCs were initially observed in small clusters in *Lox-K-ras* lung tumors, representing a small proportion of the total tumor cell population that largely consisted of SP-C^{pos} cells (Jackson et al., 2001). We reasoned that tumor DPCs might originate from a cell population in the adult lung similar to embryonic lung epithelial precursors that are positive for Clara and AT2 cell markers (Wuenschell et al., 1996). Therefore, sections of wild-type lung were examined by dual immunofluorescence (IF) for CCA and SP-C. As shown in Figure 1, DPCs were identified in normal lung at the BADJ. As expected, CCA staining was present in columnar bronchiolar and terminal bronchiolar cells, whereas SP-C staining was limited to AT2 cells and DPCs. Upon examination of more than 100 terminal bronchioles from five wild-type mice, at least one DPC was detected in 35% ± 9% of BADJs. Notably, CCA staining appeared to be less abundant in DPCs than in Clara cells. DPCs were not identified in alveolar spaces, bronchioles, large airways, or in the trachea. Rarely, DPCs were found in the proximal portion of the terminal bronchiole (data not shown). Staining for the neuroendocrine cell marker CGRP was not observed at the BADJ (data not shown). Because the data described below provide evidence that DPCs function as stem cells for Clara cells and alveolar cells, DPCs will be referred to hereafter as *b*ronchio*a*lveolar *s*tem *c*ells (BASCs).

BASCs Respond to Bronchiolar and Alveolar Injury

Identification of BASCs at the BADJ localized them in a putative stem cell niche. Previous studies showed that naphthalene-resistant Clara cells were present at the BADJ. Furthermore, the BrdU^{pos} CCA^{pos} cells identified during early airway renewal were located precisely where we identified BASCs (Giangreco et al., 2002; Hong et al., 2001; Reynolds et al., 2000a; Reynolds et al., 2000b).

To determine if airway damage affected BASCs, dual IF for CCA and SP-C was performed at various time points after naphthalene treatment. Although significant Clara cell loss was observed by 52 hr after naphthalene treatment, the number of BASCs did not significantly decrease at any time point (Figures 2A–2C and data not shown). The naphthalene-resistant population included BASCs and Clara cells. However, in some terminal bronchioles, the only cells remaining were BASCs (data not shown). IF revealed that there was a significant increase in terminal bronchioles with two or more BASCs one week after naphthalene (16% ± 5% in controls to 30% ± 9% at 1 week, $p = 0.03$; Figure 2C). Consistent with IF, FACS analysis (described below; Figure 3) showed that the abundance of BASCs did not change 24 hr after naphthalene but was 1.3-fold increased by 1 week after treatment ($p = 0.04$) (see Supplemental Data available with this article online). Six to seven weeks after naphthalene treatment, bronchiolar epithelium was restored (Giangreco et al., 2002; data not shown), and the number of BASCs per BADJ was comparable to that in untreated lung (Figure 2C).

We administered BrdU prior to euthanasia to determine if BASCs proliferated in response to naphthalene.

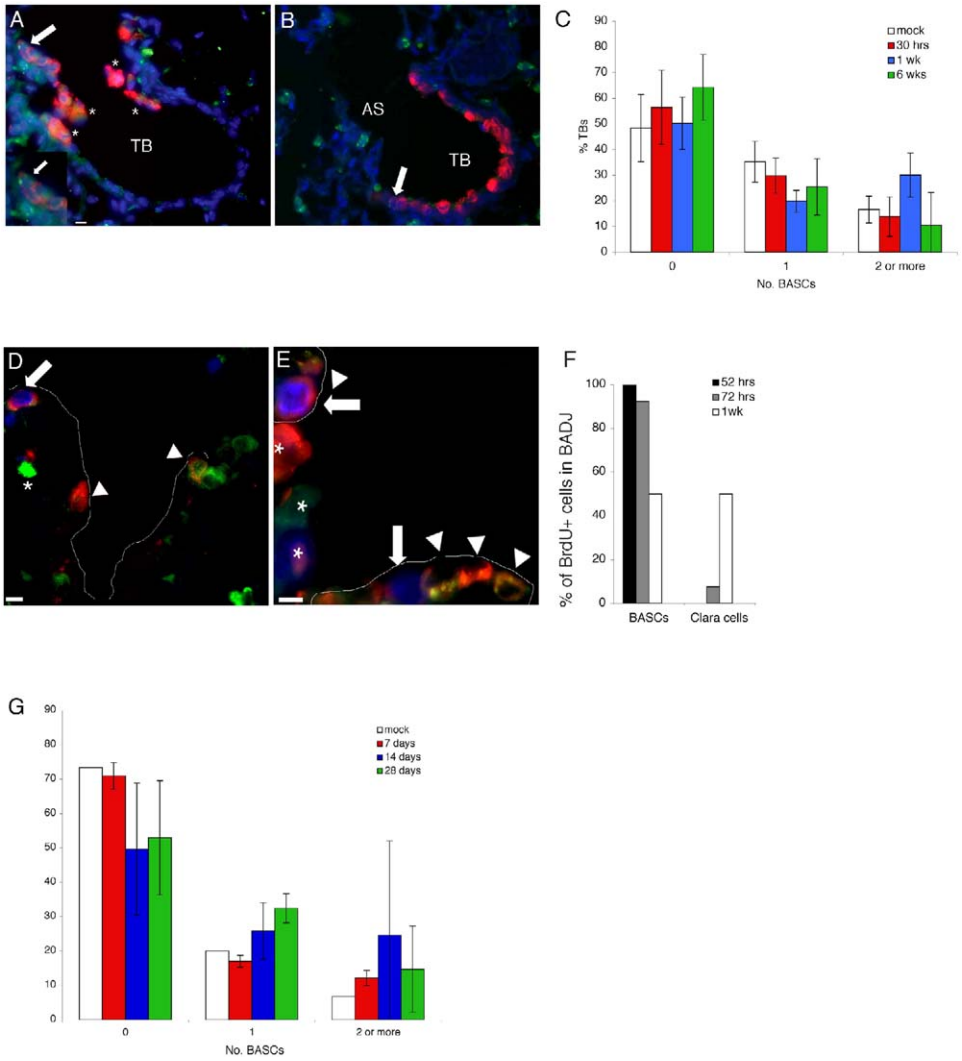

Figure 2. BASCs Are Damage Resistant and Proliferate during Epithelial Repair

(A and B) IF as in Figure 1, showing a TB from a naphthalene (A) or mock (B) treated mouse 36 hr after treatment. Arrows, BASCs. Asterisks, Clara cells sloughing off into the airway. Inset, enlarged BADJ region. All scale bars, 10 μm.

(C) The percentage of TBs containing 0, 1, and 2 or more BASCs at various time points after naphthalene is shown (mean ± SD).

(D) Four-color IF was performed to analyze proliferation after naphthalene treatment. DAPI staining (not shown) was used to identify the outline of TBs (dashed line). A TB 52 hr after naphthalene is shown with a single $BrdU^{pos}$ (blue), SP-C^{pos} (green), CCA^{pos} (red) BASC at the BADJ (arrow). Arrowheads point to a $BrdU^{neg}$ Clara cell more proximal in the TB (left) and a $BrdU^{neg}$ BASC at the other BADJ (right). Asterisk, green autofluorescence.

(E) Staining as in (D) of a TB 72 hr after naphthalene shows $BrdU^{neg}$ BASCs at the BADJ (arrowheads) situated next to $BrdU^{pos}$ CCA^{pos} SP-C^{neg} cells (arrows). Asterisks, cells sloughing off into the airway.

(F) The percentage of $BrdU^{pos}$ cells at the BADJ contributed by SP-C^{pos} CCA^{pos} cells (BASCs) or SP-C^{neg} CCA^{pos} cells (Clara cells) at various time points after naphthalene treatment is shown. Data are from at least 100 BrdU-positive cells for each time point.

(G) The percentage of TBs containing 0, 1, and 2 or more BASCs (mean ± SD) at various time points after bleomycin is shown.

In the BADJ, $BrdU^{pos}$ cells were first detected at 52 hr after naphthalene, and all were SP-C^{pos} CCA^{pos} (Figures 2D and 2F). Seventy-two hours after naphthalene, CCA^{pos} SP-C^{neg} $BrdU^{pos}$ cells were present adjacent to $BrdU^{neg}$ BASCs (Figures 2E and 2F), suggesting that they arose from BASCs. $BrdU^{pos}$ cells in the nonterminal bronchiolar epithelium at all time points were CCA^{pos} SP-C^{neg}, consistent with the report of distinct stem cell niches in proximal and terminal bronchioles (Giangreco et al., 2002). BASCs were $BrdU^{neg}$ in normal, untreated lung (data not shown), whereas they proliferated during airway repair and were $BrdU^{neg}$ after its completion.

Since these data pointed to a role for BASCs in terminal bronchiolar cell maintenance, we next determined whether BASCs were also important in response to alveolar damage. Bleomycin was administered intranasally, and at various time points after treatment, the incidence of BASCs was determined. Similar to their response to naphthalene, BASC numbers increased af-

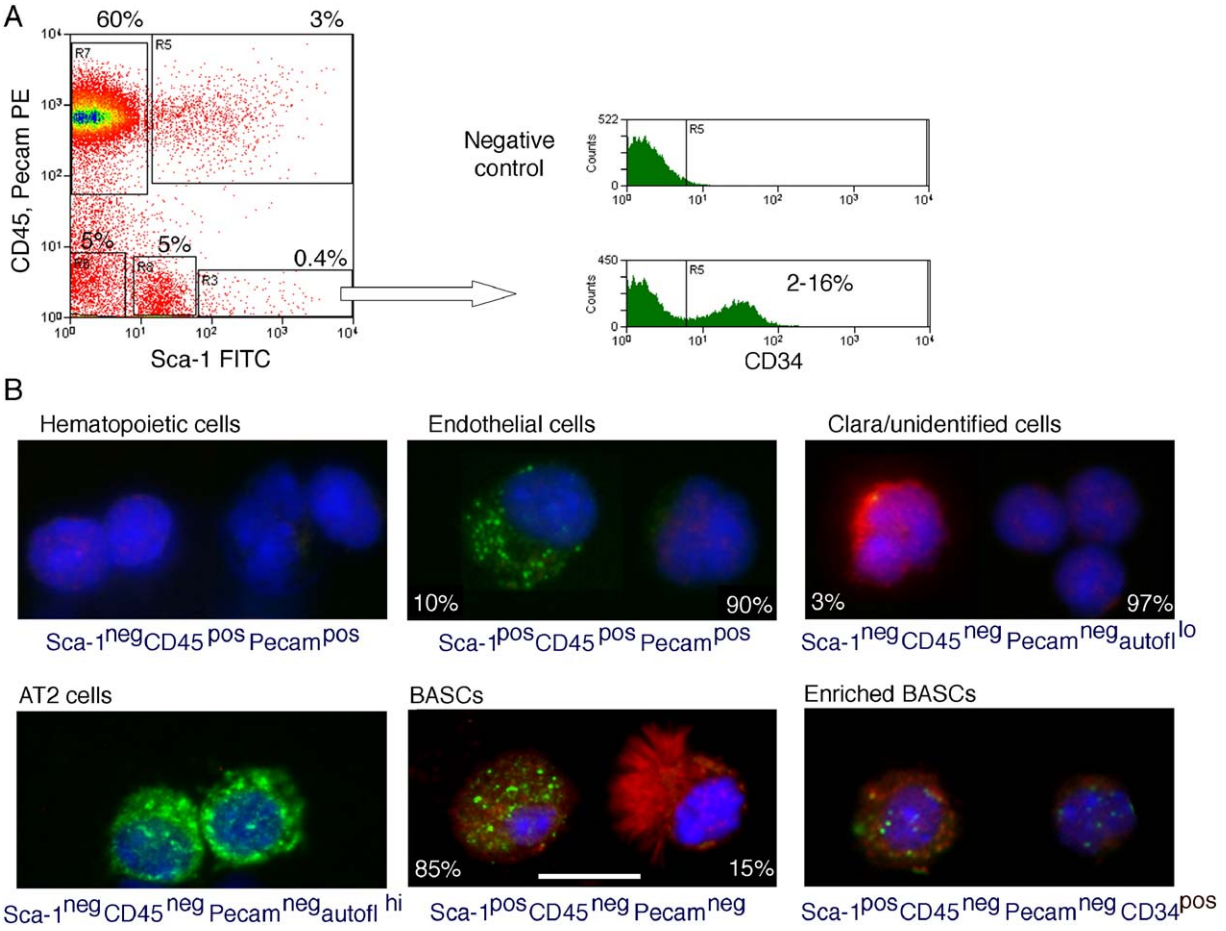

Figure 3. FACS Methodology to Isolate BASCs

(A) Typical scatter plot showing the distinct cellular populations in lung identified by staining for Sca-1, CD45, and Pecam. The percentage of total lung represented by each population is indicated. Histograms show the percentage of cells positive for CD34 in a negative control (no CD34 antibody) (top) and in the Sca-1^{pos} CD45^{neg} Pecam^{neg} population (bottom).

(B) IF (as in other figures) of the indicated populations for CCA and SP-C after sorting and cytospin. The percentage of cells exhibiting the representative staining pattern is 100% unless otherwise indicated. autofl^{hi}, cells with high green autofluorescence without Sca-1 staining. Scale bar, 10 μm.

ter bleomycin treatment. Significant increases were observed 14 days after bleomycin ($p = 0.01$), when AT1 cell depletion became evident in previous studies (Aso et al., 1976). In contrast, BASC distribution was significantly different neither at 7 days after treatment, before substantial alveolar damage was documented, nor after 28 days, when effective repair is complete or long-term damage is apparent (Aso et al., 1976; Figure 2G).

Together, these data suggested that BASCs play a role in both bronchiolar and alveolar cell injury repair and homeostasis.

Isolation of BASCs

Based on their staining for AT2 and Clara cell-specific markers, their response to damage in vivo, and their location at the bifurcation between bronchiolar and respiratory epithelium, we hypothesized that BASCs constitute a stem or progenitor cell population that maintains Clara cells and AT2 cells in adult lung. To explore this hypothesis, it was necessary to isolate and further characterize BASCs. As CCA and SP-C are cytoplasmic, intracellular markers, they were not suitable for live cell isolation of BASCs by FACS. Due to its presence on the surface of hematopoietic stem cells and mammary-gland progenitors (Morrison and Weissman, 1994 and references within; Welm et al., 2002), Sca-1 was considered to be a potential marker of BASCs.

We developed the following protocol for purification of BASCs by FACS. Fresh lung cells were prepared, red blood cells were removed by lysis, and the hematopoietic and endothelial lineages were excluded by virtue of the fact that they are positive for CD45 and Pecam, respectively. From the remaining cells, Sca-1^{pos} cells were sorted to determine if they contained the BASC population (Figure 3). This population represented 0.4% of the total lung cell preparation in 4- to 8-week-old wild-type mice (Figure 3A). Immunophenotyping of the FACS-sorted populations using the CCA and SP-C markers determined that only the Sca-1^{pos} CD45^{neg} Pecam^{neg} population contained BASCs (Figure 3B).

Eighty-five percent of these cells were CCA^{pos} SP-C^{pos} cells, whereas 15% were CCA^{pos} ciliated cells. The Sca-1^{neg} CD45^{neg} Pecam^{neg} population with high autofluorescence was comprised of SP-C^{pos} CCA^{neg} AT2 cells and represented 5%–20% of the total lung population. The Sca-1^{neg} CD45^{neg} Pecam^{neg} population with low autofluorescence contained CCA^{pos} Clara cells and other unidentified cells. The Sca-1^{neg} CD45^{pos} Pecam^{pos} population was composed of hematopoietic cells, including macrophages. The Sca-1^{pos} CD45^{pos} Pecam^{pos} population contained mostly endothelial cells, and 10% was composed of highly autofluorescent, Pecam^{neg} Sca-1^{neg} AT2 cells (data not shown).

BASCs were purified further based on positive staining for CD34, a known marker of skin epithelial and hematopoietic stem cells, (Blanpain et al., 2004; Ramalho-Santos et al., 2002; Ivanova et al., 2002; Tumbar et al., 2004; Morris et al., 2004). Two to sixteen percent of Sca-1^{pos} CD45^{neg} Pecam^{neg} cells were positive for CD34 (Figure 3A). Whereas the Sca-1^{pos} CD45^{neg} Pecam^{neg} CD34^{neg} population contained ciliated cells and CCA^{pos} SP-C^{pos} cells (data not shown), all cells in the Sca-1^{pos} CD45^{neg} Pecam^{neg} CD34^{pos} population were positive for CCA and SP-C, and no ciliated cells were present (Figure 3B). Thus, the Sca-1^{pos} CD45^{neg} Pecam^{neg} CD34^{pos} population was further enriched for BASCs.

To verify the anatomical location of the cells selected using this FACS isolation scheme, we performed IF for CCA, Sca-1, and CD34 on lung tissue sections. Sca-1 and CD34 were detected in endothelial cells in capillaries and larger blood vessels. All Sca-1^{pos} cells in bronchioles were CD34^{neg} ciliated cells, whereas Sca-1^{pos} cells in terminal bronchioles were at the BADJ and were CCA^{pos} (Supplemental Data and data not shown). CD34 staining was detected in some Clara cells in bronchioles (Supplemental Data). Importantly, Sca-1^{pos} CD34^{pos} CCA^{pos} cells were located exclusively at the BADJ (Supplemental Data). To determine if these cells were of hematopoietic origin, sections were also stained for the marker CD45. The CD34^{pos} cells were negative for CD45 (Supplemental Data). These data suggested that use of Sca-1- and CD34-positive surface staining, together with exclusion of hematopoietic and endothelial lineage, allows for the isolation of the same BADJ cells identified by IF for CCA and SP-C. Together, these results provided a FACS methodology sufficient to isolate live lung cell populations and compare their ability to self-renew and differentiate in culture.

BASCs Exhibit Stem Cell Properties in Culture

Lung epithelial cells harvested using this FACS protocol formed colonies after 1 week when grown on feeders (Figure 4A). All cells in feeder-grown colonies from BASC cultures were CCA^{pos} SP-C^{pos}, suggesting that growth on feeders maintained the cells' undifferentiated state. Eighty percent of colonies on feeders from total lung cultures also contained CCA^{pos} SP-C^{pos} cells, but in all colonies examined, these cells were only a portion of the colony. The remainder of total lung colonies contained CCA^{neg} SP-C^{pos} cells. Thus, the colonies present in total lung cultures likely arose from a mixture of AT2 cells, BASCs, and other unidentified cells, an important note for subsequent analyses of total lung cultures. As expected, AT2 cultures only contained SP-C^{pos} cells (Supplemental Data).

Several methods were used to show that the colonies arising from BASC cultures were clonal. First, 5% of single-cell cultures of Sca-1^{pos} CD45^{neg} Pecam^{neg} CD34 ^{pos} cells plated on feeders formed epithelial colonies identical to those arising from multiple Sca-1^{pos} CD45^{neg} Pecam^{neg} cells (Figure 4A). Plating of neither single AT2 cells nor single total lung cells produced colonies. Second, limiting dilution analysis revealed that the BASC population is 5.5-fold enriched for single cells that can give rise to colonies. There was a linear relationship between the cell density and the number of colonies generated from total lung or BASCs but not those generated from AT2 cells (Figure 4B). Limiting dilution showed that 1 out of 452 total lung cells gave rise to a colony, whereas the clonal frequency was 1 out of 81 for the Sca-1^{pos} CD45^{neg} Pecam^{neg} population. Finally, plating mixtures of GFP^{pos} BASCs from D4/XEGFP mice, which carry an X-linked GFP transgene (Hadjantonakis et al., 1998), with GFP^{neg} BASCs from wild-type mice only yielded entirely GFP^{pos} or GFP^{neg} colonies (Supplemental Data). In contrast, mixtures of GFP^{pos} and GFP^{neg} AT2 cells and total lung cells produced mixed colonies (containing GFP^{pos} and GFP^{neg} cells), suggesting that the majority of their colonies were not clonal; these data are consistent with IF and limiting dilution results (Supplemental Data).

In addition to clonal colony formation, only BASCs exhibited extensive self-renewal in culture (Figure 4C). Single-cell suspensions from individual colonies in primary total lung and BASC cultures formed colonies identical to primary cell colonies (Figure 4A and data not shown), whereas AT2 cultures did not produce secondary colonies. Total lung cell cultures failed to produce colonies in tertiary cultures, perhaps owing to the use of nonclonal colonies (above). In contrast, the Sca-1^{pos} CD45^{neg} Pecam^{neg} population has been passaged up to nine times to date without diminution of colony-forming ability (Figure 4C and data not shown).

BASCs also had a greater capacity for differentiation than other lung epithelial cells (Figure 4D). By 4 days on Matrigel, Sca-1^{pos} CD45^{neg} Pecam^{neg} cells formed three-dimensional structures containing a central cluster of ~400 cells with surrounding cells exhibiting short cytoplasmic extensions. By 7 days, the cytoplasmic extensions were more complex and resembled alveolar epithelium. Total lung cell cultures produced similar structures, whereas AT2 cultures remained in small clusters. Furthermore, Sca-1^{pos} CD45^{neg} Pecam^{neg} CD34^{pos} BASC cultures appeared identical to those isolated without CD34 selection (compare images in Figure 4D).

Immunophenotyping of Matrigel cell cultures with CCA, SP-C, and aquaporin-5 (AQ5), a marker of AT1 cells (Nielsen et al., 1997), confirmed the multilineage differentiation capacity of BASCs. Seven- to ten-day-old total lung cell and BASC cultures contained CCA^{pos} SP-C^{neg} cells (Clara-like cells), SP-C^{pos} CCA^{neg} cells (AT2-like cells), and AQ5^{pos} cells (AT1-like cells) (Figure 4). Cells with the most abundant SP-C staining were located around the periphery of the cell clusters in

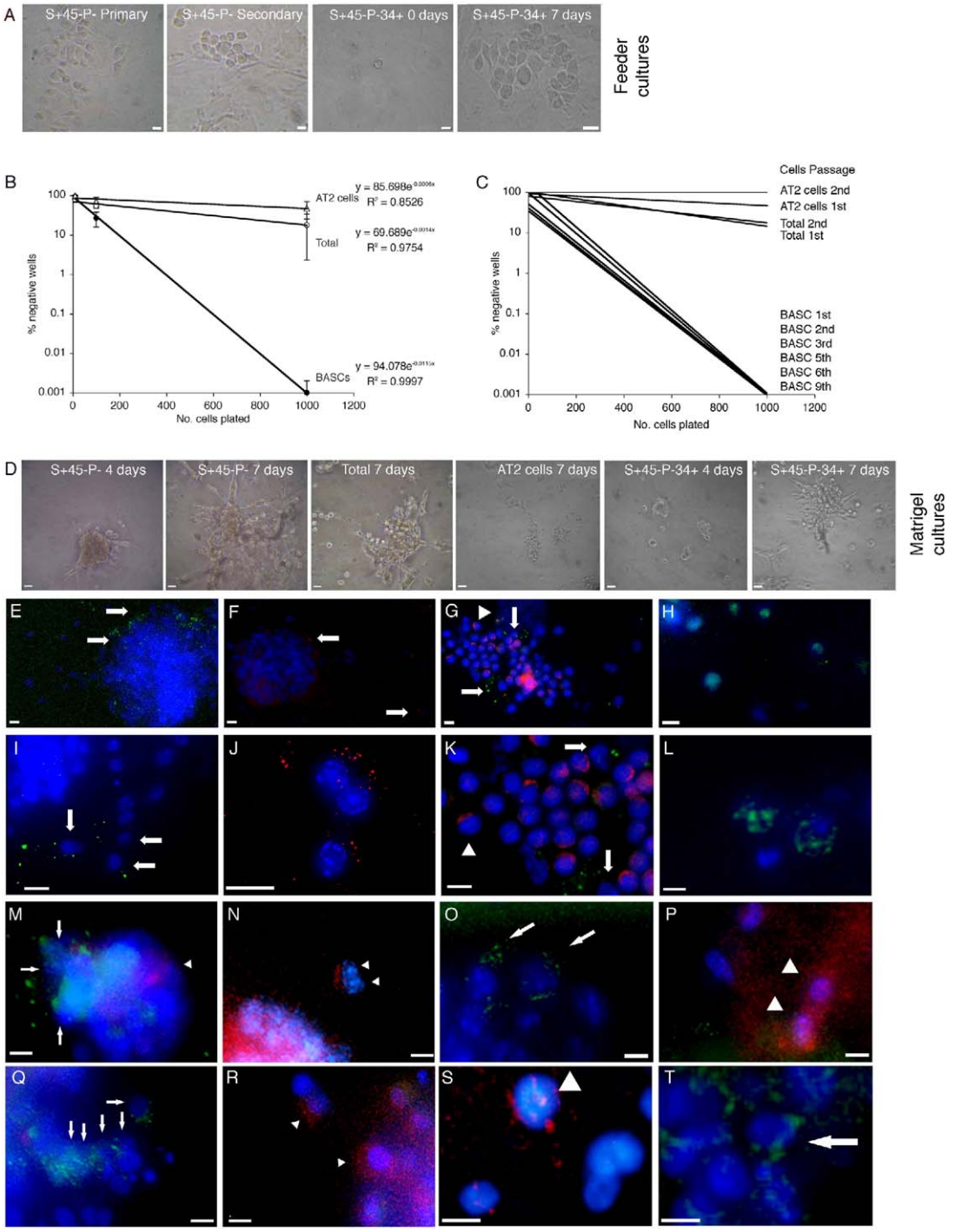

Figure 4. BASCs Self-Renew and Are Multipotent

(A) Phase-contrast images of colonies resulting from (left to right) feeder-cultured BASCs, secondary BASC culture, a single Sca-1^{pos} CD45^{neg} Pecam^{neg} CD34^{pos} cell plated on day 0, and its resulting colony after 1 week.

(B) Limiting dilution analysis comparing AT2 cells, total unsorted lung, and BASCs. The percentage of wells without colony formation for the corresponding number of plated cells is shown with the coefficient and formula from regression analysis. Data from three independent experiments (mean ± SD) were used.

(C) Limiting dilution analysis of serially passaged cells.

(D) Representative phase-contrast images of Matrigel-cultured Sca-1^{pos} CD45^{neg} Pecam^{neg} cells (S+45–P–), total lung, AT2 cells, and Sca-1^{pos} CD45^{neg} Pecam^{neg} CD34^{pos} cells (S+45–P–34+).

(E–T) Cultures grown on Matrigel were subjected to IF for SP-C (green) and CCA (red) (E, G, I, K, M–T) or SP-C (green) and AQ5 (red) (F, H, J, L) and analyzed by deconvolution microscopy to assess differentiation. All scale bars, 10 μm. Images represent similar results from at least three independent experiments.

BASC cultures (Figures 4E and 4I). The cells extending from the core cluster and exhibiting cytoplasmic branching reminiscent of AT1 cells were AQ5^{pos}, as were rare cells on the periphery of the clusters (Figures 4F and 4J). Dissociation of the clusters revealed that they contained Clara-like and AT2-like cells (Figures 4G and 4K). FACS further confirmed the differentiation status of cells in Matrigel cultures (Supplemental Data). BASC cultures contained AT2 cells (25%–84% of the culture), Clara/other unidentified cells (28%–70%), and BASCs (0.36%–3.3%). Total lung cultures consisted of Clara/other unidentified cells, AT2 cells, and endothelial cells but no BASCs. AT2 cell cultures retained the AT2 cell population and did not produce BASCs.

In our analyses, 100% of BASC cultures were multipotent, producing Clara- and AT2-like cells. In contrast, 25% of total lung cultures were multipotent, 50% produced AT2-like cells only, and 25% produced Clara-like cells only. AT2 cell cultures did not exhibit differentiation (Figures 4H and 4L). Importantly, 100% of colonies derived from single BASCs gave rise to both Clara- and AT2-like cells on Matrigel (n = 6, representing three independent experiments) (Figures 4M–4P). Furthermore, even after eight passages, BASC clones produced Clara- and AT2-like cells, showing that they retained differentiation capacity while undergoing self-renewal (Figures 4Q–4T). No ciliated cells were detected at any time point of culturing based on morphology and staining with antisera raised against acetylated tubulin (data not shown), suggesting that ciliated cells present in the sorted Sca-1^{pos} CD45^{neg} Pecam^{neg} population (Figure 3) did not survive culture conditions or contribute to differentiation and other culture characteristics.

Together, data from lung cell cultures demonstrated that BASCs are able to self-renew and possess multilineage differentiation potential.

BASCs Are Expanded in Lung Tumorigenesis

Identification of BASCs at the BADJ placed them at a putative site of tumorigenesis, supporting the hypothesis that BASCs may be important in lung adenocarcinoma initiation. Serial section analysis indicated that *Lox-K-ras* adenomas often arose near terminal bronchioles. In fact, lesions present at early time points after oncogenic K-ras activation appeared to be continuations of bronchiolar hyperplasia and alveolar hyperplasia arising in terminal bronchioles (Jackson et al., 2001).

Supporting their role in tumorigenesis, IF showed that BASC numbers were increased in the earliest tumorigenic lesions in *Lox-K-ras* mice. Whereas the majority of wild-type terminal bronchioles contained one to three BASCs with or without AdCre (Figures 5A and 5C), up to four BASCs at a single BADJ were detected 1 week after AdCre in 2% of *Lox-K-ras* terminal bronchioles (Figures 5B and 5C). The distribution of BASCs continued to increase 2 weeks after AdCre; seven BASCs were observed at single BADJs, and 16% of TBs had four to seven BASCs ($p = 1.7e^{-6}$ compared to wild-type controls) (Figure 5C). Verifying IF results, a 3.6-fold increase in BASCs in *Lox-K-ras* mice was observed by FACS analysis 5 days after AdCre administration ($p = 0.009$) (Supplemental Data). These data show that BASC expansion was coincident with the formation of AAH, the precursor lesion for adenocarcinoma (Jackson et al., 2001). Furthermore, delivery of increased titer of AdCre, which resulted in increased tumor number (Jackson et al., 2001), was also correlated to an increase in BASC incidence ($p = 1.7e^{-12}$; Figure 5D), linking BASC expansion to tumor number. BASC numbers further increased during tumor progression; 37% of *Lox-K-ras* terminal bronchioles had four to eight BASCs 6 weeks after Cre ($p = 5.4e^{-6}$; Figure 5C) and BASCs were also expanded 12 weeks after Cre ($p = 1.3e^{-6}$; Figure 5E).

Consistent with BASC expansion being a key, early event in tumorigenesis, we observed a specific effect of K-ras G12D activation on the proliferation and differentiation of BASCs. *LSL-K-ras G12D* BASC cultures treated with AdCre underwent a 2.5-fold expansion in cell number compared to control cultures ($p = 0.05$; Figure 6A). In contrast, AdCre-infected AT2 cultures did not show a significant change in cell number. AdCre-infected BASC cultures exhibited reduced differentiation; the percentage of Matrigel-grown BASC cultures composed of Sca-1^{pos} CD45^{neg} Pecam^{neg} cells was 4-fold increased compared to AdEmpty-infected cultures, there was a 1.6-fold increase in AT2 cells, and a decrease in other cells was observed (Figure 6B). These findings were similar to the changes in abundance of BASCs and AT2 cells observed by FACS after K-ras G12D activation in vivo (Supplemental Data). Importantly, BASCs did not arise in AdCre-treated AT2 cell cultures. Our observations were not due to inherent differences in ability to infect BASC and AT2 cell cultures, as they exhibited similar efficiency for recombination of the *K-ras* allele (Figure 6C). These data suggested that the first outcome of K-ras G12D activation on lung epithelia is an expansion of BASC number and subsequent differentiation toward the alveolar lineage.

BASC Stimulation In Vivo Affects Tumorigenesis

We reasoned that we could further dissect the cellular requirements for adenocarcinoma formation by combining K-ras G12D activation with naphthalene treatment, which stimulates proliferation of BASCs in vivo (see Figure 2). *LSL-K-ras G12D* mice and wild-type con-

(E–L) BASC cultures contained SP-C^{pos} CCA^{neg} cells (arrows in [E] and [G], enlarged in [I] and [K]), AQ5^{pos} cells (arrows in [F], enlarged in [J]), and SP-C^{neg} CCA^{pos} cells (arrowheads in [G], enlarged in [K]). Only SP-C^{pos} cells were present in AT2 cell cultures ([H], enlarged in [L]).
(M–P) Differentiated cells derived from a single Sca-1^{pos} CD45^{neg} Pecam^{neg} CD34^{pos} cell were SP-C^{pos} CCA^{neg} (arrows) (M and O) or SP-C^{neg} CCA^{pos} cells (arrowheads) (N and P). Cells in (M) and (N) were derived from a single cell, and cells in (O) and (P) were derived from another single cell.
(Q–T) Single cells on the periphery of clusters derived from fifth (Q and R) or eighth (S and T) passage BASCs were SP-C^{pos} CCA^{neg} (arrows) (Q and T) or SP-C^{neg} CCA^{pos} cells (arrowheads) (R and S).

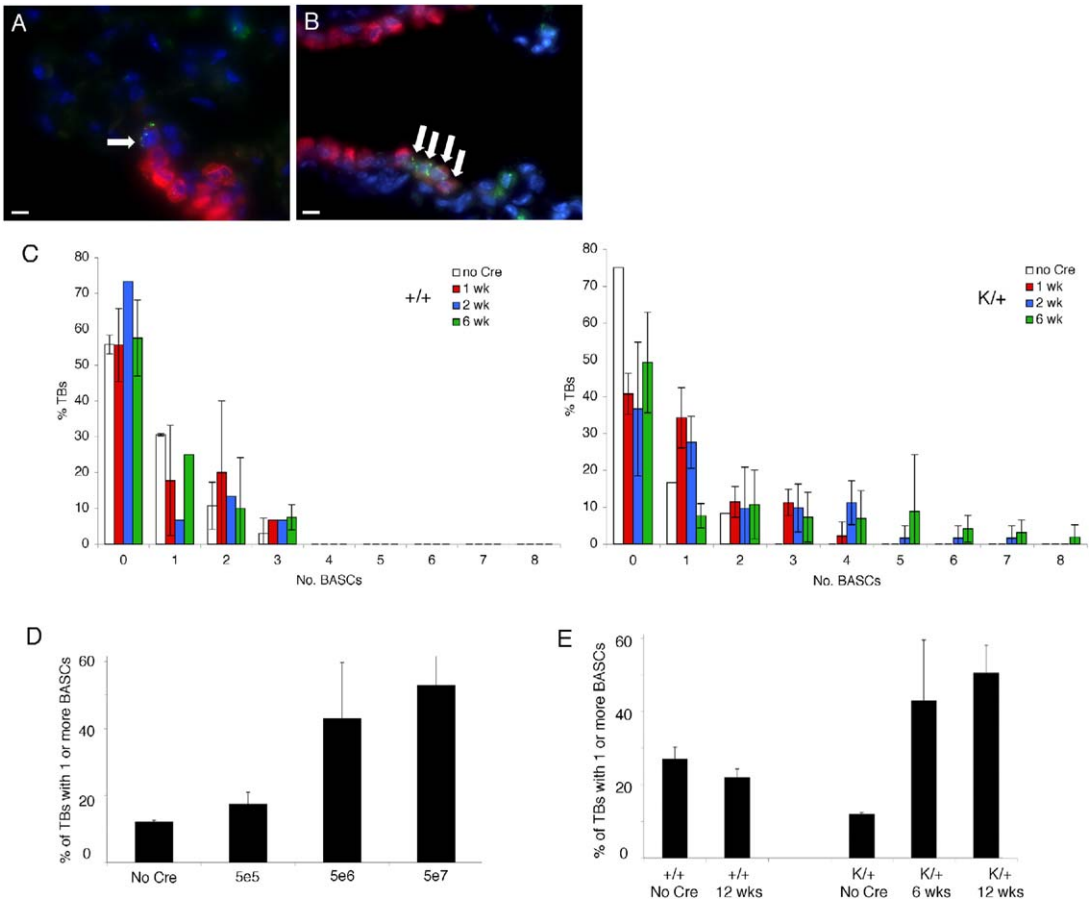

Figure 5. BASC Expansion in Adenocarcinoma Precursors and Tumors

All bar graphs show mean ± SD.

(A and B) IF for CCA and SP-C as in other figures, from wild-type (A) and *Lox-K-ras* (B) mice 1 week after AdCre. Expanded numbers of BASCs (arrows) are observed in *Lox-K-ras* lung. Images, 400×; scale bars, 10 μm.

(C) Distribution of BASC number at time points indicated after AdCre. The percentage of TBs containing one to eight BASCs is shown for wild-type (+/+, left) and *Lox-K-ras* (K/+, right) lungs.

(D) The percentage of *Lox-K-ras* TBs with at least one BASC detected for each AdCre dose (particle-forming units/ml).

(E) The percentage of TBs with at least one BASC in *Lox-K-ras* mice (K/+) compared to wild-type mice (+/+) is shown for each condition.

trols were treated with naphthalene, tumorigenesis was initiated by administering AdCre 24 hr to 3 days later, and mice were euthanized after 6 weeks to determine tumor incidence and size.

Naphthalene administration resulted in an increase in tumor number and area, further implicating BASCs in tumor initiation. In three independent experiments, naphthalene treatment was correlated with an increase in tumor number; 1.3-, 2.2-, and 2.3-fold more tumors were observed in *Lox-K-ras* mice treated with naphthalene before AdCre compared to controls ($p = 0.04$; Figure 7A). An even greater impact on tumor area was associated with naphthalene treatment; adenomas comprised a 6-, 12-, and 15-fold greater proportion of total lung area when initiated after airway damage in the three experiments ($p = 0.009$; Figure 7B). Importantly, increased tumorigenicity was not attributable to more effective AT2 cell infection after naphthalene treatment. Infection with AdGFP followed by IF for SP-C or CCA 24 hr later indicated that there was no significant increase in the incidence of GFP^{pos} AT2 cells in control versus naphthalene-treated animals (7.8% versus 10.5% of infected cells were $SP\text{-}C^{pos}$).

Discussion

We have identified a cell population in the adult mouse lung that has properties of stem cells and is linked to lung tumor initiation. Wild-type BASCs were found in a putative stem cell niche, proliferated during epithelial repair in vivo, and were capable of multipotent differentiation and self-renewal in culture. We suggest that BASCs are a regional stem cell population in the distal lung. Increases in BASC number were observed in *Lox-K-ras* mice with AAH and adenomas. The temporal and spatial correlation of BASC expansion with early-stage lesions suggests that AAH arise from transformed BASCs. Stimulation of BASCs by airway injury resulted in an increase in tumor number and size, further implicating BASCs in tumorigenesis.

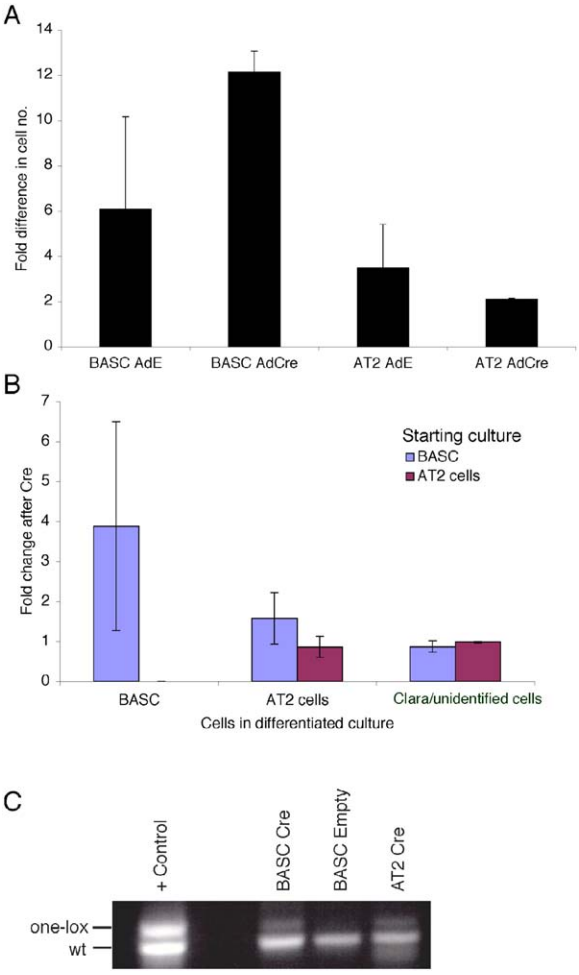

Figure 6. Specific Effect on BASC Cultures after K-ras G12D Activation

(A) The fold change in the number of cells (mean ± SD) present after culture and infection with Adeno Empty (AdE) or Adeno Cre (AdCre) is shown for *LSL-K-ras G12D* BASC and AT2 cell cultures. Cell number was determined by FACS.

(B) The fold change in the percentage of the total population (AdCre/AdE) represented by BASCs, AT2 cells, and Clara/unidentified cells, determined by FACS (mean ± SD).

(C) PCR to assess recombination in infected BASC or AT2 cell cultures. wt, product amplified from wild-type allele; one-lox, product from recombined *Lox-K-ras* allele; + control, DNA from a *Lox-K-ras* tumor.

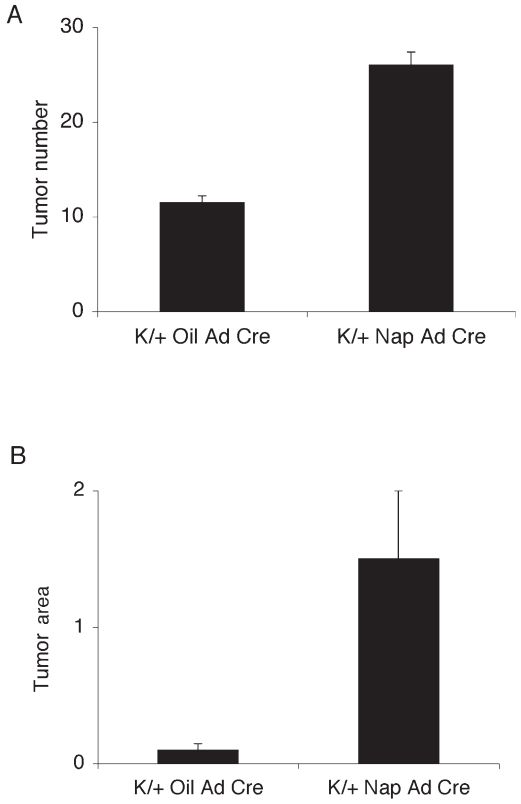

Figure 7. Cooperation between Naphthalene Treatment and *K-ras* Tumorigenesis In Vivo

Tumor number (A) and tumor area (B) (calculated as the ratio of tumor area to lung area) in *Lox-K-ras* mice (K/+) after treatment with naphthalene prior to infection (Nap Ad Cre), compared to controls treated with corn oil only (Oil Ad Cre), are shown. Data are the mean ± SD from one of three independent experiments that had similar results.

Defining Lung Stem Cells

Our data illustrate that BASCs are bona fide stem cells that share characteristics with previously defined adult stem cell populations (Blanpain et al., 2004; Chiasson et al., 1999; Doetsch et al., 1999; Johansson et al., 1999; Kruger et al., 2002; Morris et al., 2004; Tropepe et al., 2000). Importantly, we have shown that cultured BASCs exhibit proliferative capacity and self-renewal and are multipotent in clonal assays. BASCs have retained these properties over eight passages to date.

As studies identifying populations with stem cell properties from solid adult tissues emerge, it is becoming increasingly important to define precise criteria for stem cell terminology. For example, it is currently debated whether an essential part of the definition of a stem cell is the ability to reconstitute the majority of a tissue upon reintroduction in vivo or if it is sufficient to demonstrate comparable properties in cell culture. Ascribing stem cell characteristics to a cell population without evidence for differentiation and self-renewal in vivo may weaken the term "stem cells" (Seaberg and van der Kooy, 2003), but, in fact, rather few reports of stem cell populations have been supported by in vivo data. Furthermore, some studies that include in vivo data have relied on expansion of putative stem cells in culture prior to engraftment, raising the possibility that culturing changed the potency of the isolated cell population (Blanpain et al., 2004; Gage et al., 1995; Spangrude et al., 1995).

We acknowledge that the ultimate test for stem cell activity is a single-cell clonogenic transplantation assay, as has been done in the hematopoietic system (Krause et al., 2001; Osawa et al., 1996). However, such assays are particularly challenging when applied to stem cells of epithelial tissues. Epithelial cells are closely associated with endothelial cells, stromal fibroblasts, inflammatory cells, and accompanying extracel-

lular matrix and cell-cell interactions. Some or all of these components may be required to allow survival, engraftment, and proper differentiation of putative stem and progenitor cells. Although there is an established protocol to test for mammary epithelial stem cells without injection of additional exogenous supporting cells (Deome et al., 1959; Hoshino and Gardner, 1967; Welm et al., 2002), a comparable system remains to be created for other epithelial tissues, including the lung.

It will be crucial to formally determine the ability of BASCs to produce differentiated lung epithelia and self-renew in vivo to further define their functions. It remains possible that BASCs may function more similarly to progenitor cells, rather than stem cells, in an in vivo setting; further, the BASC population we isolated may contain a mixture of stem and progenitor cells. Although there is an assay for reconstitution of denuded trachea subcutaneously implanted into immunodeficient mice, this system provides a tracheal-like environment rather than mimicking the distal lung region (Delplanque et al., 2000). Bone-marrow cells may contribute to lung tissue after damage (Harris et al., 2004; Kotton et al., 2001; Krause et al., 2001), but it is unlikely that stem cells normally residing in the lung can survive conditions in circulation and home properly to the BADJ. Therefore, experiments to test stem cell function of BASCs may require introduction precisely to their original niche. This will likely involve introduction of genetically marked BASCs into the respiratory system of wild-type mice after bronchiolar or alveolar cell damage. Alternatively, it would be informative to genetically label endogenous BASCs or other epithelial cells specifically in vivo after lung damage and track their progeny without introduction of exogenous cells. Such studies would define the lineage relationships that exist between adult lung epithelial cells but will require additional knowledge of BASC-, progenitor cell-, and differentiated cell-specific markers.

Current evidence supports the existence of multiple stem cell niches in the lung (Otto, 2002). Our work suggests that BASCs are a stem cell population for distal lung epithelia with potentiality limited to Clara, AT2, and AT1 cells. Their location in the BADJ places BASCs next to each of the niches in which their putative progeny reside (the terminal bronchiole for Clara cells and the alveolar space for AT2 cells). Furthermore, BASCs are normally in a quiescent state and can be activated in response to bronchiolar and alveolar injury in vivo.

The expansion of BASCs during airway renewal was subtle, leading us to hypothesize that BASCs give rise to a progenitor population, perhaps a subtype of Clara cells, that restores damaged terminal bronchiolar epithelium. BASCs were the first cells to proliferate in response to naphthalene, and they comprised the majority of the proliferating population up to 1 week after damage. $BrdU^{pos}$ Clara cells were situated next to $BrdU^{neg}$ BASCs at later stages of terminal bronchiolar repair, consistent with the hypothesis that they arose from BASCs.

BASCs may also give rise to an alveolar progenitor population to maintain alveolar homeostasis in vivo, given their response to bleomycin treatment. Although the commonly held view has been that AT2 cells are progenitors for AT1 cells because cultured AT2 cells acquire AT1-like properties in culture (Isakson et al., 2001), our data suggest that BASCs give rise to AT1 cells. Alternatively, BASCs may give rise to AT2 cells, which, in turn, produce AT1 cells. Interestingly, the results of Aso et al. suggest that there may be two niches that mediate alveolar repair; both proliferation of AT2 cells in alveolar spaces and expansion and differentiation of some bronchiolar cells was observed after bleomycin-mediated damage (Aso et al., 1976). Furthermore, Daly et al. found that SP-C and CC10 coexpression was present in a subset of distal bronchiolar cells following bleomycin-mediated lung injury and proposed that this finding may be evidence for a stem cell population in bronchioles that responds to alveolar damage nearby (Daly et al., 1997; Daly et al., 1998).

Elucidating Lung Cancer Cells of Origin

Our work provides the first evidence that stem cells are the target cell population in lung adenocarcinoma. Prior work from Dick, Weissman, and colleagues has provided compelling evidence that stem cells can be the target cells in tumorigenesis for hematopoietic malignancies (Bonnet and Dick, 1997; Cozzio et al., 2003; Passegue et al., 2004). Importantly, BASCs were expanded at early stages of tumorigenesis in vivo and exhibited the first proliferative response following K-ras G12D activation in culture. We have also observed BASC expansion in association with lung tumorigenesis initiated by expression of a point mutant p53 allele (Olive et al., 2004), ruling out a specific effect of AdCre on BASC expansion (data not shown). Since Clara cells or AT2 cells are widely thought to be the precursor cells in adenocarcinoma, this work points to an alternative model of the cell of origin for this subtype of lung cancer. Although we found expanded numbers of BASCs in early lesions, we have not yet shown that BASCs are necessary for tumor development and maintenance. It is conceivable that a progenitor cell population that gains the property of self-renewal may be equally capable of supporting tumor initiation (Cozzio et al., 2003).

We hypothesize that lung tumors arise from expansion of stem cells and that advanced tumors retain characteristics of differentiated lineage(s) due to influences from the microenvironment or continued oncogenic signaling. For example, expansion of BASCs stimulated by oncogenic K-ras and continued proliferation in the context of constitutive K-ras signaling may result in adenocarcinomas largely composed of AT2 cells. Our analysis of the effect of activated K-ras on BASC differentiation in culture supports this reasoning. Further, we found that most cells in *Lox-K-ras* tumors were $SP\text{-}C^{pos}$ CCA^{neg}, and some tumor cells were also positive for AQ5 (Jackson et al., 2001; data not shown); the immunophenotype of *Lox-K-ras* tumors matches the alveolar differentiation pattern we observed for BASCs. It is likely that a corresponding human BASC population exists, and it too may play a role in adenocarcinoma development. This would account for the fact that adenocarcinomas most frequently resemble bronchiolar and alveolar components of normal human lung (Rosai and Sobin, 1995).

Identification of the BASC population, its niche, and a means to isolate and propagate this population lends

promise to a better understanding of the cellular and molecular mechanisms of lung development, homeostasis, and disease. Chronic lung diseases could theoretically be alleviated by directed differentiation of lung stem cells to restore defective lung epithelia. These cells may also be used for ex vivo gene therapy of genetic diseases affecting the lung such as cystic fibrosis. Regarding lung cancer, BASCs were detected in established tumors, suggesting that they may contribute continuously to tumor development and progression. Tumor-associated BASCs may constitute a tumor stem cell population similar to those that have been defined in breast and brain cancers (Al-Hajj et al., 2003; Reya et al., 2001; Singh et al., 2003; Singh et al., 2004) and, as such, may be a critical target for anticancer therapy. Finally, additional studies pointing to a role for BASCs in tumor initiation may fuel more effective early-identification markers and chemoprevention strategies for lung cancer by specifically targeting hyperproliferative BASCs in the early stage of disease.

Experimental Procedures

Mice and Tissues

Lox-stop-lox K-ras G12D mice (Jackson et al., 2001) and wild-type littermates were maintained in viral-free conditions on an F1 129 SvJ/C57Bl6 background. Four- to eight-week-old mice were used for FACS or intranasal infections as described (Jackson et al., 2001). Naphthalene (Aldrich) was dissolved in Mazola corn oil and injected i.p. at 275 mg/kg using sex- and background-matched control mice. Bleomycin (Sigma; 40 μl of 1.88 U/ml in PBS) was administered intranasally. 30 mg/kg BrdU in PBS was injected i.p. 2 hr before euthanasia for proliferation studies. Tissue preparation was as described (Jackson et al., 2001). BASCs were quantified by scoring sections from at least three mice for each condition. Bioquant Software was used to quantify tumor area.

FACS Analysis

Single-cell suspensions from lung were prepared as described with modifications (Bortnick et al., 2003; see also Supplemental Data). Sca-1-FITC, CD45.1-Biotin, Pecam-Biotin, CD34-PE, and Streptavidin-PE were from Pharmingen. 7AAD (Molecular Probes) staining eliminated dead cells. Cell sorting was performed with a Cytomation MoFlo, and data were analyzed with Cytomation Summit software.

Immunofluorescence

Immunostaining of tissues and cells was performed as previously described (Jackson et al., 2001) using antisera raised against mouse CCA (gift); proSP-C (RDI); proSP-C clone 7705, CC10, CD34 clone C-18, and aquaporin 5 (Santa Cruz); proSP-C (Chemicon clone 3786); CGRP and acetylated tubulin (Sigma); CD34 Mec14.7 (Abcam); Sca-1 (R&D Systems); BrdU (Becton Dickinson); and donkey Alexafluore secondary antibodies (Molecular Probes). Sorted or cultured cells were stained after cytospin at 600 rpm for 3 min and fixation and permeabilization with CytoFix/CytoPerm (Pharmingen). Triple-color microscopy and imaging were performed with a Nikon Eclipse E600 and a Spot cooled CCD camera and software. Four-color microscopy and deconvolution were performed with a Zeiss Axioplan II, cooled CCD camera, and OpenLab software. Images were processed with Adobe Photoshop.

Epithelial Cultures

Cells were plated in DME/HEPES/10% FBS on 96-well plates coated with 100 μl Matrigel (Becton Dickinson) or irradiated DR4 MEFs. Matrigel cultures were fixed on plates or treated with collagenase/dispase for cytospin, IF, and FACS. For limiting dilution analysis, 1, 10, 100, or 1000 cells were sorted onto feeders to assess colony formation 1 week later. Regression analysis was performed to calculate the x value at which the y value is 37%, which correlates with each colony arising from a single cell (Tropepe et al., 2000). For serial passage, wells containing a single colony were trypsinized, and single cell suspensions were plated onto fresh feeder-coated wells for the next passage. Colony number was assessed after 1 week, and the process was repeated. Matrigel cultures were infected with $1e^6$ PFU AdCre or AdEmpty after 1–3 days in culture and analyzed by FACS 7 days later.

Statistics

Statistical analyses were performed using Mstat software (Norman Drinkwater, McArdle Laboratory for Cancer Research, University of Wisconsin). For comparison of the distribution of BASC number per terminal bronchiole, the Cochran-Armitage test was performed, and data with a trend p value of 0.05 or less were considered significant. Other analyses were done using the Wilcoxon rank sum test or Fisher's exact test as appropriate.

Supplemental Data

Supplemental Data include Supplemental Experimental Procedures and five figures and are available with this article online at http://www.cell.com/cgi/content/full/121/6/823/DC1/.

Acknowledgments

The CCA antibody was a generous gift from A. Mukherjee from the NICHD/NIH. X-linked GFP mice were kindly provided by the Jaenisch Lab. The authors thank M. Brown, M. Jennings, M. Xie, G. Paradis, and M. Perry for excellent technical assistance; B. Stripp and A. Giangreco for helpful suggestions; and J. Neilson and Jacks Lab members for critical reading of the manuscript. C.F.B.K. is a Merck Fellow of The Jane Coffin Childs Memorial Fund for Medical Research. T.J. is a Howard Hughes Medical Institute Investigator.

Received: June 30, 2004
Revised: December 22, 2004
Accepted: March 31, 2005
Published: June 16, 2005

References

Al-Hajj, M., Wicha, M.S., Benito-Hernandez, A., Morrison, S.J., and Clarke, M.F. (2003). Prospective identification of tumorigenic breast cancer cells. Proc. Natl. Acad. Sci. USA *100*, 3983–3988.

Aso, Y., Yoneda, K., and Kikkawa, Y. (1976). Morphologic and biochemical study of pulmonary changes induced by bleomycin in mice. Lab. Invest. *35*, 558–568.

Bannister, L.H. (1999). Respiratory system. In Gray's Anatomy, P.L. Williams, R. Warwick, M. Dyson, and L.H. Bannister, eds. (New York: Churchill Livingstone), pp. 1666–1672.

Blanpain, C., Lowry, W.E., Geoghegan, A., Polak, L., and Fuchs, E. (2004). Self-renewal, multipotency, and the existence of two cell populations within an epithelial stem cell niche. Cell *118*, 635–648.

Bonnet, D., and Dick, J.E. (1997). Human acute myeloid leukemia is organized as a hierarchy that originates from a primitive hematopoietic cell. Nat. Med. *3*, 730–737.

Borthwick, D.W., Shahbazian, M., Krantz, Q.T., Dorin, J.R., and Randell, S.H. (2001). Evidence for stem-cell niches in the tracheal epithelium. Am. J. Respir. Cell Mol. Biol. *24*, 662–670.

Bortnick, A.E., Favari, E., Tao, J.Q., Francone, O.L., Reilly, M., Zhang, Y., Rothblat, G.H., and Bates, S.R. (2003). Identification and characterization of rodent ABCA1 in isolated type II pneumocytes. Am. J. Physiol. Lung Cell. Mol. Physiol. *285*, L869–L878.

Chiasson, B.J., Tropepe, V., Morshead, C.M., and van der Kooy, D. (1999). Adult mammalian forebrain ependymal and subependymal cells demonstrate proliferative potential, but only subependymal cells have neural stem cell characteristics. J. Neurosci. *19*, 4462–4471.

Cozzio, A., Passegue, E., Ayton, P.M., Karsunky, H., Cleary, M.L., and Weissman, I.L. (2003). Similar MLL-associated leukemias aris-

ing from self-renewing stem cells and short-lived myeloid progenitors. Genes Dev. *17*, 3029–3035.

Daly, H.E., Baecher-Allan, C.M., Barth, R.K., D'Angio, C.T., and Finkelstein, J.N. (1997). Bleomycin induces strain-dependent alterations in the pattern of epithelial cell-specific marker expression in mouse lung. Toxicol. Appl. Pharmacol. *142*, 303–310.

Daly, H.E., Baecher-Allan, C.M., Paxhia, A.T., Ryan, R.M., Barth, R.K., and Finkelstein, J.N. (1998). Cell-specific gene expression reveals changes in epithelial cell populations after bleomycin treatment. Lab. Invest. *78*, 393–400.

Delplanque, A., Coraux, C., Tirouvanziam, R., Khazaal, I., Puchelle, E., Ambros, P., Gaillard, D., and Peault, B. (2000). Epithelial stem cell-mediated development of the human respiratory mucosa in SCID mice. J. Cell Sci. *113*, 767–778.

Deome, K.B., Faulkin, L.J., Jr., Bern, H.A., and Blair, P.B. (1959). Development of mammary tumors from hyperplastic alveolar nodules transplanted into gland-free mammary fat pads of female C3H mice. Cancer Res. *19*, 515–520.

Dermer, G.B. (1982). Origin of bronchioloalveolar carcinoma and peripheral bronchial adenocarcinoma. Cancer *49*, 881–887.

Doetsch, F., Caille, I., Lim, D.A., Garcia-Verdugo, J.M., and Alvarez-Buylla, A. (1999). Subventricular zone astrocytes are neural stem cells in the adult mammalian brain. Cell *97*, 703–716.

Gage, F.H., Coates, P.W., Palmer, T.D., Kuhn, H.G., Fisher, L.J., Suhonen, J.O., Peterson, D.A., Suhr, S.T., and Ray, J. (1995). Survival and differentiation of adult neuronal progenitor cells transplanted to the adult brain. Proc. Natl. Acad. Sci. USA *92*, 11879–11883.

Giangreco, A., Reynolds, S.D., and Stripp, B.R. (2002). Terminal bronchioles harbor a unique airway stem cell population that localizes to the bronchoalveolar duct junction. Am. J. Pathol. *161*, 173–182.

Giangreco, A., Shen, H., Reynolds, S.D., and Stripp, B.R. (2003). Molecular phenotype of airway side population cells. Am. J. Physiol. Lung Cell. Mol. Physiol. *286*, L624–L630. 10.1152/ajplung.00149.2003

Goodell, M.A., Brose, K., Paradis, G., Conner, A.S., and Mulligan, R.C. (1996). Isolation and functional properties of murine hematopoietic stem cells that are replicating in vivo. J. Exp. Med. *183*, 1797–1806.

Gunning, W.T., Stoner, G.D., and Goldblatt, P.J. (1991). Glyceraldehyde-3-phosphate dehydrogenase and other enzymatic activity in normal mouse lung and in lung tumors. Exp. Lung Res. *17*, 255–261.

Hadjantonakis, A.K., Gertsenstein, M., Ikawa, M., Okabe, M., and Nagy, A. (1998). Non-invasive sexing of preimplantation stage mammalian embryos. Nat. Genet. *19*, 220–222.

Harris, R.G., Herzog, E.L., Bruscia, E.M., Grove, J.E., Van Arnam, J.S., and Krause, D.S. (2004). Lack of a fusion requirement for development of bone marrow-derived epithelia. Science *305*, 90–93.

Hong, K.U., Reynolds, S.D., Giangreco, A., Hurley, C.M., and Stripp, B.R. (2001). Clara cell secretory protein-expressing cells of the airway neuroepithelial body microenvironment include a label-retaining subset and are critical for epithelial renewal after progenitor cell depletion. Am. J. Respir. Cell Mol. Biol. *24*, 671–681.

Hoshino, K., and Gardner, W.U. (1967). Transplantability and life span of mammary gland during serial transplantation in mice. Nature *213*, 193–194.

Isakson, B.E., Lubman, R.L., Seedorf, G.J., and Boitano, S. (2001). Modulation of pulmonary alveolar type II cell phenotype and communication by extracellular matrix and KGF. Am. J. Physiol. Cell Physiol. *281*, C1291–C1299.

Ivanova, N.B., Dimos, J.T., Schaniel, C., Hackney, J.A., Moore, K.A., and Lemischka, I.R. (2002). A stem cell molecular signature. Science *298*, 601–604.

Jackson, E.L., Willis, N., Mercer, K., Bronson, R.T., Crowley, D., Montoya, R., Jacks, T., and Tuveson, D.A. (2001). Analysis of lung tumor initiation and progression using conditional expression of oncogenic K-ras. Genes Dev. *15*, 3243–3248.

Johansson, C.B., Momma, S., Clarke, D.L., Risling, M., Lendahl, U., and Frisen, J. (1999). Identification of a neural stem cell in the adult mammalian central nervous system. Cell *96*, 25–34.

Kotton, D.N., Ma, B.Y., Cardoso, W.V., Sanderson, E.A., Summer, R.S., Williams, M.C., and Fine, A. (2001). Bone marrow-derived cells as progenitors of lung alveolar epithelium. Development *128*, 5181–5188.

Krause, D.S., Theise, N.D., Collector, M.I., Henegariu, O., Hwang, S., Gardner, R., Neutzel, S., and Sharkis, S.J. (2001). Multi-organ, multi-lineage engraftment by a single bone marrow-derived stem cell. Cell *105*, 369–377.

Kruger, G.M., Mosher, J.T., Bixby, S., Joseph, N., Iwashita, T., and Morrison, S.J. (2002). Neural crest stem cells persist in the adult gut but undergo changes in self-renewal, neuronal subtype potential, and factor responsiveness. Neuron *35*, 657–669.

Mason, R.J., Kalina, M., Nielsen, L.D., Malkinson, A.M., and Shannon, J.M. (2000). Surfactant protein C expression in urethane-induced murine pulmonary tumors. Am. J. Pathol. *156*, 175–182.

Minna, J.D., Roth, J.A., and Gazdar, A.F. (2002). Focus on lung cancer. Cancer Cell *1*, 49–52.

Mori, M., Chiba, R., and Takahashi, T. (1993). Atypical adenomatous hyperplasia of the lung and its differentiation from adenocarcinoma. Characterization of atypical cells by morphometry and multivariate cluster analysis. Cancer *72*, 2331–2340.

Mori, M., Rao, S.K., Popper, H.H., Cagle, P.T., and Fraire, A.E. (2001). Atypical adenomatous hyperplasia of the lung: a probable forerunner in the development of adenocarcinoma of the lung. Mod. Pathol. *14*, 72–84.

Morris, R.J., Liu, Y., Marles, L., Yang, Z., Trempus, C., Li, S., Lin, J.S., Sawicki, J.A., and Cotsarelis, G. (2004). Capturing and profiling adult hair follicle stem cells. Nat. Biotechnol. *22*, 411–417.

Morrison, S.J., and Weissman, I.L. (1994). The long-term repopulating subset of hematopoietic stem cells is deterministic and isolatable by phenotype. Immunity *1*, 661–673.

Nielsen, S., King, L.S., Christensen, B.M., and Agre, P. (1997). Aquaporins in complex tissues. II. Subcellular distribution in respiratory and glandular tissues of rat. Am. J. Physiol. *273*, C1549–C1561.

Olive, K.P., Tuveson, D.A., Ruhe, Z.C., Yin, B., Willis, N.A., Bronson, R.T., Crowley, D., and Jacks, T. (2004). Mutant p53 gain of function in two mouse models of Li-Fraumeni syndrome. Cell *119*, 847–860.

Osawa, M., Hanada, K., Hamada, H., and Nakauchi, H. (1996). Long-term lymphohematopoietic reconstitution by a single CD34-low/negative hematopoietic stem cell. Science *273*, 242–245.

Otto, W.R. (2002). Lung epithelial stem cells. J. Pathol. *197*, 527–535.

Passegue, E., Wagner, E.F., and Weissman, I.L. (2004). JunB deficiency leads to a myeloproliferative disorder arising from hematopoietic stem cells. Cell *119*, 431–443.

Ramalho-Santos, M., Yoon, S., Matsuzaki, Y., Mulligan, R.C., and Melton, D.A. (2002). "Stemness": transcriptional profiling of embryonic and adult stem cells. Science *298*, 597–600.

Reya, T., Morrison, S.J., Clarke, M.F., and Weissman, I.L. (2001). Stem cells, cancer, and cancer stem cells. Nature *414*, 105–111.

Reynolds, S.D., Giangreco, A., Power, J.H., and Stripp, B.R. (2000a). Neuroepithelial bodies of pulmonary airways serve as a reservoir of progenitor cells capable of epithelial regeneration. Am. J. Pathol. *156*, 269–278.

Reynolds, S.D., Hong, K.U., Giangreco, A., Mango, G.W., Guron, C., Morimoto, Y., and Stripp, B.R. (2000b). Conditional clara cell ablation reveals a self-renewing progenitor function of pulmonary neuroendocrine cells. Am. J. Physiol. Lung Cell. Mol. Physiol. *278*, L1256–L1263.

Rosai, J., and Sobin, L.H. (1995). Conditional clara cell ablation reveals a self-renewing progenitor function of pulmonary neuroendocrine cells. In Atlas of Tumor Pathology (Washington, DC: Armed Forces Institute of Pathology).

Seaberg, R.M., and van der Kooy, D. (2003). Stem and progenitor cells: the premature desertion of rigorous definitions. Trends Neurosci. *26*, 125–131.

Singh, S.K., Clarke, I.D., Terasaki, M., Bonn, V.E., Hawkins, C., Squire, J., and Dirks, P.B. (2003). Identification of a cancer stem cell in human brain tumors. Cancer Res. *63*, 5821–5828.

Singh, S.K., Hawkins, C., Clarke, I.D., Squire, J.A., Bayani, J., Hide, T., Henkelman, R.M., Cusimano, M.D., and Dirks, P.B. (2004). Identification of human brain tumour initiating cells. Nature *432*, 396–401.

Spangrude, G.J., Brooks, D.M., and Tumas, D.B. (1995). Long-term repopulation of irradiated mice with limiting numbers of purified hematopoietic stem cells: in vivo expansion of stem cell phenotype but not function. Blood *85*, 1006–1016.

Summer, R., Kotton, D.N., Sun, X., Ma, B., Fitzsimmons, K., and Fine, A. (2003). Side population cells and Bcrp1 expression in lung. Am. J. Physiol. Lung Cell. Mol. Physiol. *285*, L97–104.

Thaete, L.G., and Malkinson, A.M. (1991). Cells of origin of primary pulmonary neoplasms in mice: morphologic and histochemical studies. Exp. Lung Res. *17*, 219–228.

Tropepe, V., Coles, B.L., Chiasson, B.J., Horsford, D.J., Elia, A.J., McInnes, R.R., and van der Kooy, D. (2000). Retinal stem cells in the adult mammalian eye. Science *287*, 2032–2036.

Tumbar, T., Guasch, G., Greco, V., Blanpain, C., Lowry, W.E., Rendl, M., and Fuchs, E. (2004). Defining the epithelial stem cell niche in skin. Science *303*, 359–363.

Welm, B.E., Tepera, S.B., Venezia, T., Graubert, T.A., Rosen, J.M., and Goodell, M.A. (2002). Sca-1(pos) cells in the mouse mammary gland represent an enriched progenitor cell population. Dev. Biol. *245*, 42–56.

Wikenheiser, K.A., Clark, J.C., Linnoila, R.I., Stahlman, M.T., and Whitsett, J.A. (1992). Simian virus 40 large T antigen directed by transcriptional elements of the human surfactant protein C gene produces pulmonary adenocarcinomas in transgenic mice. Cancer Res. *52*, 5342–5352.

Wuenschell, C.W., Sunday, M.E., Singh, G., Minoo, P., Slavkin, H.C., and Warburton, D. (1996). Embryonic mouse lung epithelial progenitor cells co-express immunohistochemical markers of diverse mature cell lineages. J. Histochem. Cytochem. *44*, 113–123.